

## Article

# Impact of Ventilation Strategy on the Transmission of Outdoor Pollutants into Indoor Environment Using CFD

Murtaza Mohammadi  and John Calautit \* 

Department of Architecture and Built Environment, University of Nottingham, Nottingham NG7 2RD, UK; murtaza.mohammadi1@nottingham.ac.uk

\* Correspondence: john.calautit1@nottingham.ac.uk; Tel.: +44-7780-3531-63

**Abstract:** The transition to remote working due to the pandemic has accentuated the importance of clean indoor air, as people spend a significant portion of their time indoors. Amongst the various determinants of indoor air quality, outdoor pollution is a significant source. While conventional studies have certainly helped to quantify the long-term personal exposure to pollutants and assess their health impact, they have not paid special attention to the mechanism of transmission of pollutants between the two environments. Nevertheless, the quantification of infiltration is essential to determine the contribution of ambient pollutants in indoor air quality and its determinants. This study evaluates the transmission of outdoor pollutants into the indoor environment using 3D computational fluid dynamics modelling with a pollution dispersion model. Naturally ventilated buildings next to an urban canyon were modelled and simulated using Ansys Fluent and validated against wind tunnel results from the Concentration Data of Street Canyons database. The model consisted of two buildings of three storeys each, located on either side of a road. Two line-source pollutants were placed in the street, representing traffic emissions. Three internal rooms were selected and modelled on each floor and implemented with various ventilation strategies. Results indicate that for a canyon with an aspect ratio of 1, indoor spaces in upstream buildings are usually less polluted than downstream ones. Although within the canyon, pollution is 2–3 times higher near the upstream building. Cross ventilation can minimise or prevent infiltration of road-side pollutants into indoor spaces, while also assisting in the dispersion of ambient pollutants. The critical configuration, in terms of air quality, is single-sided ventilation from the canyon. This significantly increases indoor pollutant concentration regardless of the building location. The study reveals that multiple factors determine the indoor–outdoor links, and thorough indexing and understanding of the processes can help designers and urban planners in regulating urban configuration and geometries for improved indoor air quality. Future works should look at investigating the influence of indoor emissions and the effects of different seasons.

**Keywords:** air pollution transmission; indoor–outdoor relation; urban canyon; computational fluid dynamics; factors of transmission



**Citation:** Mohammadi, M.; Calautit, J. Impact of Ventilation Strategy on the Transmission of Outdoor Pollutants into Indoor Environment Using CFD. *Sustainability* **2021**, *13*, 10343. <https://doi.org/10.3390/su131810343>

Academic Editors: José Carlos Magalhães Pires and Álvaro Gómez-Losada

Received: 17 June 2021

Accepted: 9 September 2021

Published: 16 September 2021

**Publisher's Note:** MDPI stays neutral with regard to jurisdictional claims in published maps and institutional affiliations.



**Copyright:** © 2021 by the authors. Licensee MDPI, Basel, Switzerland. This article is an open access article distributed under the terms and conditions of the Creative Commons Attribution (CC BY) license (<https://creativecommons.org/licenses/by/4.0/>).

## 1. Introduction and Literature Review

Good air quality is essential for living a healthy life. Approximately 4.9 million deaths connected to indoor and outdoor air pollution occurred in 2017 [1]. As reported by the Global Burden of Disease [2], poor indoor air quality led to about 1.6 million deaths in the same year. The health impacts of polluted air have been an ongoing urban management topic for discussions, which have also been emphasised in several epidemiological studies. Accordingly, pollutants such as CO, NO<sub>2</sub>, O<sub>3</sub>, etc., can have a short- and long-term impact on both humans and animals' primary and secondary health [3,4]. Past research recognises that the reduction of air pollution will increase life expectancy considerably [5]; additionally, according to [6–8], the exposure to particulate matter (PM) increased the mortality rate of COVID-19 patients during the pandemic. Consequently, governments and institutions are advised to develop guidelines and control pollution levels.

The mode of commuting and work patterns have been greatly altered by the pandemic. Generally, people spent a significant amount of time indoors [9,10] and migration of the work environment to homes due to the lockdown has further accentuated the trend. The shift to working remotely emphasises the necessity of more studies on indoor air quality [11–15]. Therefore, the mechanism of indoor pollution and its effect on building occupants' health and well-being should be well understood and adequately assessed when designing new buildings and spaces. The activities that cause air pollution in a building include cooking, indoor heating, use of mechanical equipment, shedding from skin and/or clothes, smoking, dusting, cleaning products, etc. Outdoor–indoor air interaction also influences the transmission of pollutants between the two spaces [16]. This transmission occurs by infiltration, natural ventilation, and mechanical ventilation [17]. For indoor spaces that are naturally ventilated, one of the crucial IAQ determinants is outdoor pollution [18]. The relationship between the indoor and outdoor environment is important for visual connection, thermal regulation, and ventilation.

Environmental parameters such as meteorology, temperature difference across the building, urban landscape, spatial configuration, indoor activity, furnishings, etc., alter the rate of air exchange and consequent pollution transmission [19]. Natural ventilation relies on thermal and pressure gradients across the building façade to induce air exchange between the two domains, and attempts have been made to correlate the relationship. Multiple studies have observed that indoor PM concentration closely follows the outdoor level when the space is naturally ventilated, especially in the finer particle size range [20–22]. For instance, Zhao et al. [23] showed that average particle number concentration (PNC), in naturally ventilated German houses, followed outdoor variation during the warm season when windows were left open for a longer duration. Similarly, studies [24–26] demonstrated that indoor PM concentration in homes increased when windows were opened, and the PNC distribution curve closely followed the outdoor trend.

Air exchange due to the thermal stack effect is well established, and the buoyancy-driven airflow occurs especially in the case of single-sided ventilation [27]. This can lead to pollutants exhausted from lower levels of a building to re-enter at higher levels, and the phenomenon is amplified in low wind speed conditions [28]. However, there are multiple factors at play, and the relative contribution may significantly vary. Tippayawong [29] established a significant negative correlation between indoor PM<sub>2.5</sub> concentrations and outside temperature during the day, while, on the contrary, Lv et al. [30] found a positive relation. Similarly, there are contradictory observations related to the association between relative humidity and indoor PM<sub>2.5</sub> levels [31,32]. This is also the case for wind speed, which may be desirable in some situations and unfavourable in others. Higher wind speeds may resuspend particulate matter, increasing the aerial concentration, while it may also improve ventilation and remove particulate matter from an indoor space. It may also be size-dependent, as was indicated by Orza et al. [33]. They observed that higher wind speeds increased the concentration of particles larger than 7.5 µm and decreased the concentration for sizes smaller than 0.8 µm. Thus, there are various determinants modifying the relationship and attention must be paid to local and regional context, which may determine the dominant factor.

Another important parameter to consider is the urban context and spatial morphology of the surrounding environment. Street canyon design, building footprint, open spaces, etc., affect the dispersion of pollutants in the outdoor environment and consequently impact the indoor environment [34,35]. Ai and Mak [36] reviewed over 150 studies and indicated that deeper street canyons suffered from decoupled air flow at lower wind speeds. This leads to local recirculation in the canyon, preventing the dispersion of pollutants. This was corroborated by [37], who showed a decrease in pollution levels by increasing the permeability of the urban forms, thereby assisting the dispersion of pollutants. Urban elements such as trees, aqueducts, lamp posts, etc., can also modify air flow and alter the pollution levels [38–40]. However, the major focus of urban pollution studies has been on assessing ambient levels and inhalation exposure.

### Novelty of the Present Work

While over 450 documents were returned when searched with the following keywords, ‘pollution’ AND ‘modelling’ AND ‘urban’ AND ‘canyon’ (inclusive) on Scopus, only a few studies were investigating the transmission of outdoor pollution into indoor environments. Knowing the ambient pollution levels and the relationship between indoor and outdoor air conditions, one can estimate the IAQ and take appropriate precautionary measures. Very few studies have modelled both the indoor and outdoor environment as a combined system due to the inherent complexity and difficulty in validating the models. Tong et al. [41] investigated the pollution level inside an office space as a function of its distance from a pollutant source. The study focused only on a single isolated building next to a pollution source, and hence the impact of an upstream building on the airflow distribution and pollution concentration within the urban canyon and indoor spaces should be explored. The geometry under consideration was not an urban canyon design, which disregarded local amplification and interactions. Moreover, the pollutant was modelled as a constant flux from the inlet. Yang et al. [42] examined the impact of window opening percentage along a façade on the indoor quality of a downstream building. The work did not measure the indoor pollutant levels directly but instead chose to calculate the ventilation flux to account for IAQ. Similarly, Peng et al. [43] introduced openings in the façade of the typical canyon model to understand the dispersion characteristics of the pollution. Peng et al. [43] modelled a 2D canyon and indoor environment to assess indoor conditions. However, turbulence is essentially 3D in nature, and the finer nuances of the wind flow are not generated in a 2D flow. Some other studies which have similar objectives are listed in Table 1.

**Table 1.** Similar CFD studies investigating dispersion of urban air pollutants, and their differences w.r.t the present investigation.

Ref.	Domain	Turbulence Model	Parameter Studied	Differences w.r.t Present Investigation
[44]	An isolated building (auditorium)	Standard $k-e$	Indoor $PM_1$ , $PM_{2.5}$ , and $PM_{10}$ concentrations	A constant ambient concentration was specified at the boundary and the effect of trees was studied in modifying the indoor pollution levels.
[45]	2D canyon with a viaduct	RNG $k-e$	Indoor normalised tracer gas concentrations	A 2D canyon model including indoor domain was created and transmission of traffic pollutants was studied. Effect of temperature difference on transmission was investigated. $PM_{10}$ particles were injected into the domain, and outdoor
[46]	Several building clusters	RNG $k-e$	Normalised pollutant concentration	pollutant concentration was analysed at pedestrians’ level. Effect of urban configuration on dispersion of outdoor pollutants was studied.
[47]	Building cluster	LES and Standard $k-e$	Normalised tracer gas concentration	Outdoor dispersion of pollutant was studied for a group of buildings. Experimental and CFD simulations were carried out to assess the transmission in outdoor environment. Viral load calculations were performed for apartment
[48]	Building cluster		Tracer gas concentration	buildings and to estimate inhalation exposure of coronavirus. The study used smoke dispersion models (ATOR and CFD) to predict outdoor concentrations followed by estimating the indoor exposure by referring to established I/O ratio.

Table 1. Cont.

Ref.	Domain	Turbulence Model	Parameter Studied	Differences w.r.t Present Investigation
[49]	Isolated multiroom	SST $k-w$	H <sub>2</sub> S concentration	Indoor pollution transmission was investigated for a multiroom block. Several natural ventilation strategies were studied, and the average concentration was presented for the building.
[50]	Urban canyon	Standard $k-e$	Normalised tracer gas concentration	Transmission of outdoor pollutants into indoor domain of only the downstream building was studied. Effect of building height and arrangement was tested.
[51]	Isolated building	Baseline $k-w$	Indoor tracer gas concentration	Few window types were simulated to identify the transmission characteristics of pollutant when released from an adjacent room.
[52]	Consecutive street canyon	RNG $k-e$	Tracer gas retention time	Ventilation pattern and pollutant retention time were analysed inside a target canyon placed in the middle of a series of urban canyons. 2D and 3D models were analysed for varying street lengths.
[53]	Urban canyon	RNG $k-e$ LES	Normalised tracer gas concentration	Outdoor dispersion characteristics of traffic pollutants were studied for an isolated urban canyon.
[54]	Two industrial workshops	RNG $k-e$	Normalised tracer gas concentration	Cross-transmission of pollutants from one industrial building to another were studied under various thermal conditions.

To account for the shortcomings in previous studies, the current study developed a CFD model which adopted a modified version of the urban canyon pollution dispersion model. The present work builds upon earlier studies on pollution dispersion in street canyons [55], by integrating an indoor domain in the model. The model was validated against earlier experimental studies. The impact of the window opening pattern on the transmission of outdoor vehicular pollution into the indoor environment was studied. CFD was used to perform the simulations, as it offers a finer spatio-temporal resolution of the fluid interactions, which is often desirable for episodic contaminations, such as during a pandemic [41]. The tool is versatile and can be replicated to test various alternatives. Analytical assessment and measurement studies are unable to account for the diverse physics governing pollution dispersion and the fine resolution of measurement [56]. Unlike the previous works, the present study will be modelling a 3D urban canyon which is necessary to fully understand how the urban geometry, position of the indoor space in the building, and type of natural ventilation impacts the indoor–outdoor mean flow and pollutant transmission. The proposed model can help identify the sources of pollution issues in an urban area and provide useful guidance for future urban planning.

## 2. Materials and Methods

### 2.1. CFD Modelling and Choice of Turbulence

The choice of turbulence is often determined by the problem at hand, the focus of the investigation, and the available computational resources. While the RANS model is more often used in building studies because of its low computational cost, it cannot accurately predict the fluctuating flow field in the wake of the structure, such as separation and recirculation. LES (large eddy simulation) is a superior model, which can give better results and the transient nature of the flow field. It, however, requires higher computational resources and modelling of appropriate boundary conditions [57]. For the current study, an average concentration of pollutants within the indoor environment is needed to quantify the transmission in relation to outdoor levels. Therefore, the RANS (Reynolds-averaged Navier–Stokes) model was adopted as the predictions are within acceptable limits while

also saving computation cost, and is based on statistical averaging leading to averaged equations of mass and momentum [58]. Three different turbulence models, the  $k-\omega$  BSL, the RNG  $k-\epsilon$ , and the RSM, were used in the validation. Further analysis was carried out using RSM, as it provided the most reliable results when compared with wind tunnel results, detailed in Section 2.4.

## 2.2. Computational Domain, Mesh, and Boundary Conditions

The geometrical configuration was based on the experimental investigation by Gromke et al. [59]. The model is fairly popular and has been applied in multiple studies of pollution dispersion in urban canyons, including [44,60–62]. Detailed information pertaining to model limits and wind tunnel results are also available online [63]. The canyon consists of two cuboidal building blocks of dimensions 10, 10, and 100 m in width, height, and length, respectively. The distance between the two buildings was 10 m, representing an aspect ratio of 1. Two line-sources of pollutant were placed in the canyon. The domain consists of an outer zone and an inner sub-zone near the vicinity of the canyon with a finer mesh.

The outer domain measures 30, 24, and 8 H length, width, and height, respectively, where H is the height of the building. The building was placed 8 H away from the front boundary and 7 H from the side boundaries, leading to a blockage ratio of 5.2%. The inner domain extends 18, 3, and 5 H in width, height, and depth, respectively. The domain was discretised using hexahedral elements with several mesh sizes tested for grid independence. Mesh size was refined until no significant improvement in the results was observed. The smallest dimension of the elements in the vicinity of the canyon was 0.05 H, with at least 15 cells across the length of the smallest edge. The validation model consists of 5.2 million cells, with 1.2 million cells in the canyon. Figure 1 shows the domain description and mesh characteristics.

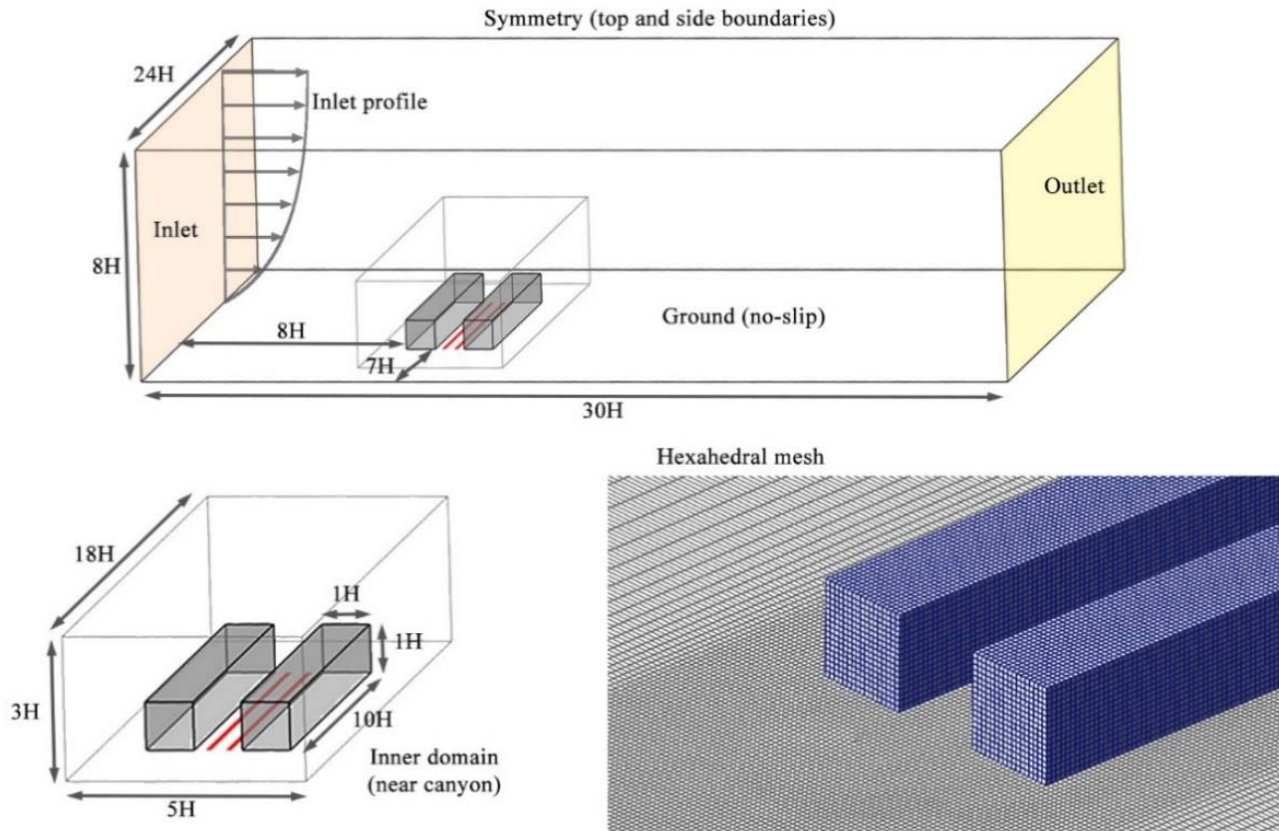


Figure 1. CFD domain, boundary condition, and surface mesh.

Inlet wind profile (speed, turbulent kinetic energy, dissipation rate profiles) was set according to the study described by [64], shown below:

$$u(z) = u_{ref} \left( \frac{z}{z_{ref}} \right)^\alpha \quad (1)$$

$$k = \frac{u_*^2}{\sqrt{C_\mu}} \left( 1 - \frac{z}{\delta} \right) \quad (2)$$

$$\varepsilon = \frac{u_*^3}{kz} \left( 1 - \frac{z}{\delta} \right) \quad (3)$$

where  $u_{ref}$  is the reference velocity equal to 4.7 m/s at a reference height  $z_{ref} = H$ .  $\delta$  is the boundary layer depth (0.5 m),  $u_*$  is the friction velocity set to 0.54 m/s. The von Karman constant ( $k$ ), and the velocity field and turbulence function ( $C_\mu$ ) were set to 0.4 and 0.09, respectively. Isothermal conditions are assumed, i.e., only wind-driven ventilation and pollution dispersion were considered. SIMPLE scheme was adopted for the pressure-velocity coupling, and second-order spatial discretisation was selected.

The tracer gas,  $SF_6$ , acted as a proxy for particulate matter and was released at the rate of  $Q = 10$  mg/s from the two-line sources (red lines in Figure 1). The measured concentration was normalised according to the formula:

$$c^+ = \frac{c * z_{ref} * u_{ref}}{Q} \quad (4)$$

### 2.3. Canyon Model with Various Configurations

The modification to the original canyon model was in the form of an indoor environment at the centre and the ends of the building, representing the extreme cases. The height of each room was  $H/3$ , and the room depth was  $H$ . The building was naturally ventilated through the windows located on either side of the room. Window dimensions were  $H/10 \times H/10$ , with sill level at 1 m above the floor. For the present case,  $H$  was set to 10 m. Walls and floors were given a thickness of 0.3 m and were accounted for in the geometry. Figure 2 shows the setup of the internal environment and its relation to the external canyon. Although it is possible to simulate all rooms in the building, the present work focused only on 18 key indoor spaces to reduce the computational time. However, additional rooms can be modelled in future works for a more detailed analysis.

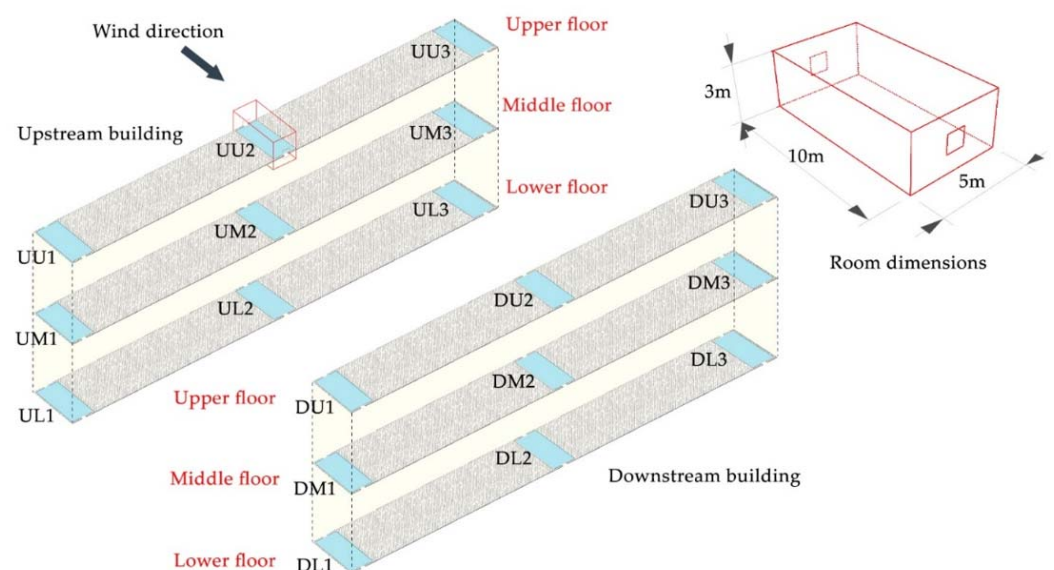


Figure 2. Location of internal spaces in the upstream and downstream buildings.

#### 2.4. Method Verification and Validation

For verification purposes, three different turbulence models, the  $k-\omega$  BSL, the RNG  $k-\epsilon$ , and the RSM were tested and compared with experimental results available on the Concentration Data of Street Canyons (CODASC) website [63] and the studies [44,64,65]. Normalised pollutant concentration values were extracted from the canyon facing walls, A and B. While Wall A is located on the upstream building, Wall B is located on the downstream building, as shown in Figure 3. The case with all windows closed was used for verification, as it represents the decoupled indoor and outdoor domain.

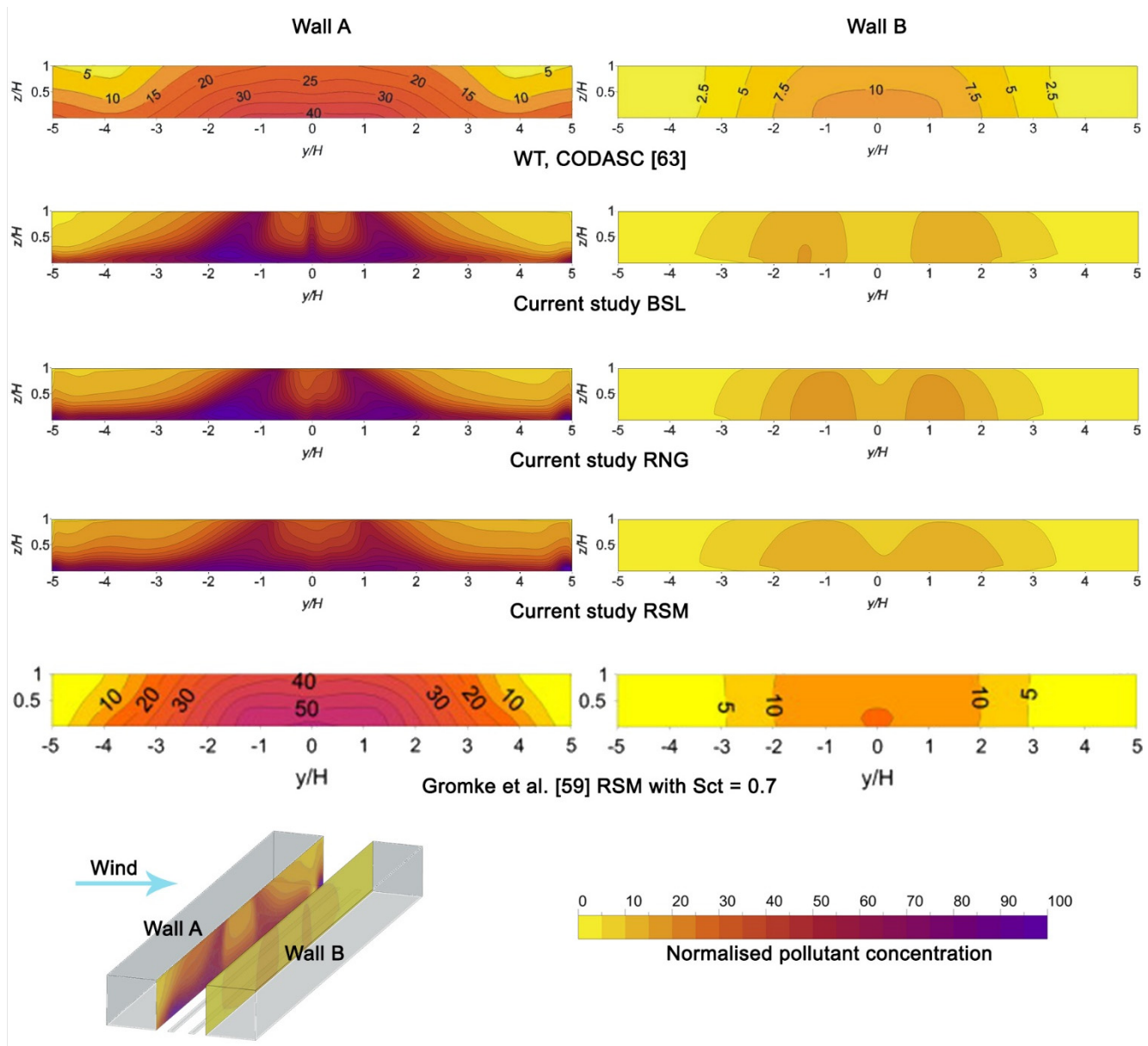


Figure 3. Validation of the pollutant concentration results against previous works [59,63].

The wind tunnel data predict the highest concentration near the centre of Wall A, especially near the bottom. The concentration gradually decreases while moving towards the corner; however, a slight increase was observed near the far end. On Wall B, the concentration decreases towards the sides; however, the magnitude of the pollution is 2–4 times lower as compared to the other wall. All three turbulence models predict similar concentration patterns, albeit with some variation. The BSL and the RNG model overpredict

SF<sub>6</sub> by 150% near the centre of Wall A, and slight underprediction (20%) occurs on the centre of Wall B. RSM also records a high pollution level near the centre and bottom of the walls, with values in the range 70–80 on Wall A. Compared with the numerical results by [55], the RSM model behaves most closely, with slight under prediction of about 33% near the centre.

Additionally, the pollutant concentration along the mid-height of the wall was also extracted, as shown in Figure 4. It was observed that while all three turbulence models overpredict pollutant concentration with respect to the wind tunnel data, the values are comparable to the numerical results by [55]. The RSM model fairly replicates the trend by [55], although studies by [65,66] are closer to the wind tunnel results. The difference in the domain settings could explain the apparent deviation. The pollutant was released at discrete points from pressure taps placed on the floor in the wind tunnel test, which were aligned along 4 parallel lines in the canyon, extending about 0.92 H beyond the building length. In the current numerical simulation, two continuous line-sources were modelled, which extend up to the canyon length.

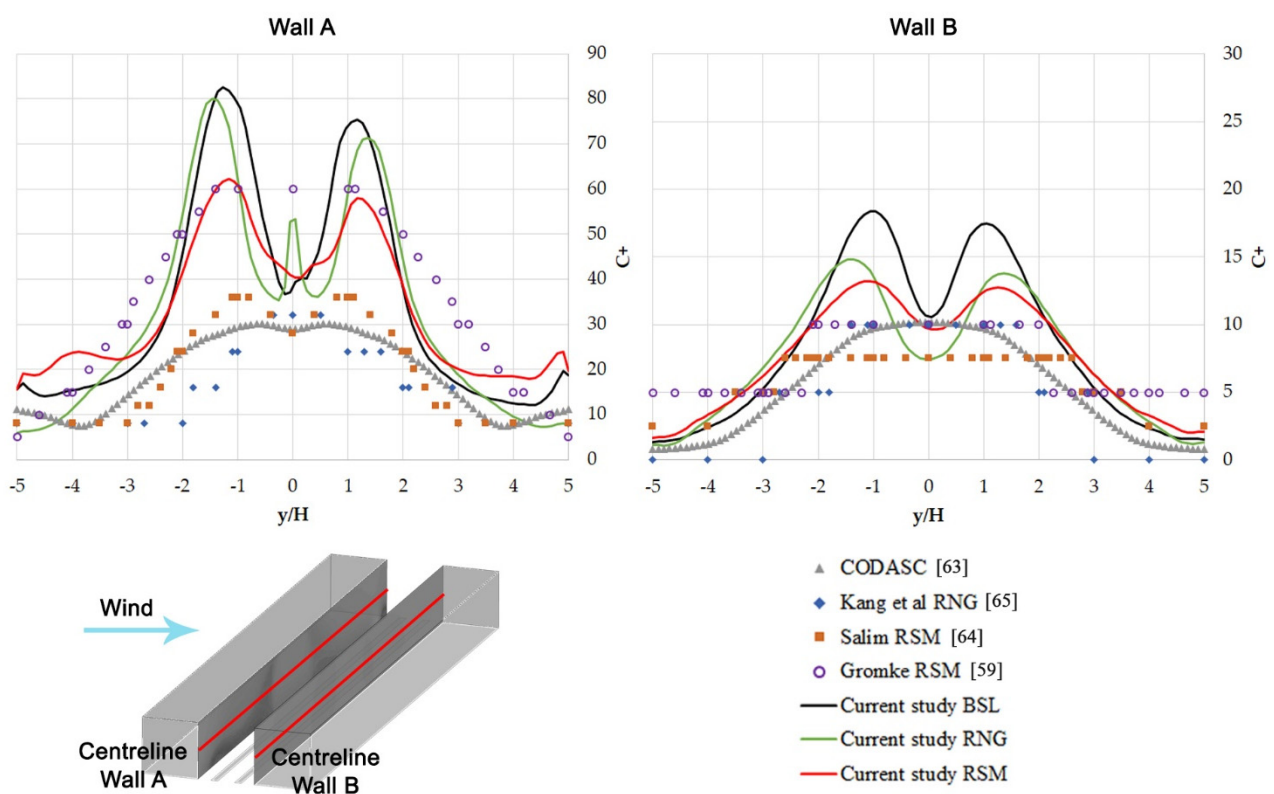


Figure 4. Validation of the pollutant concentration results against previous works [59,63–65].

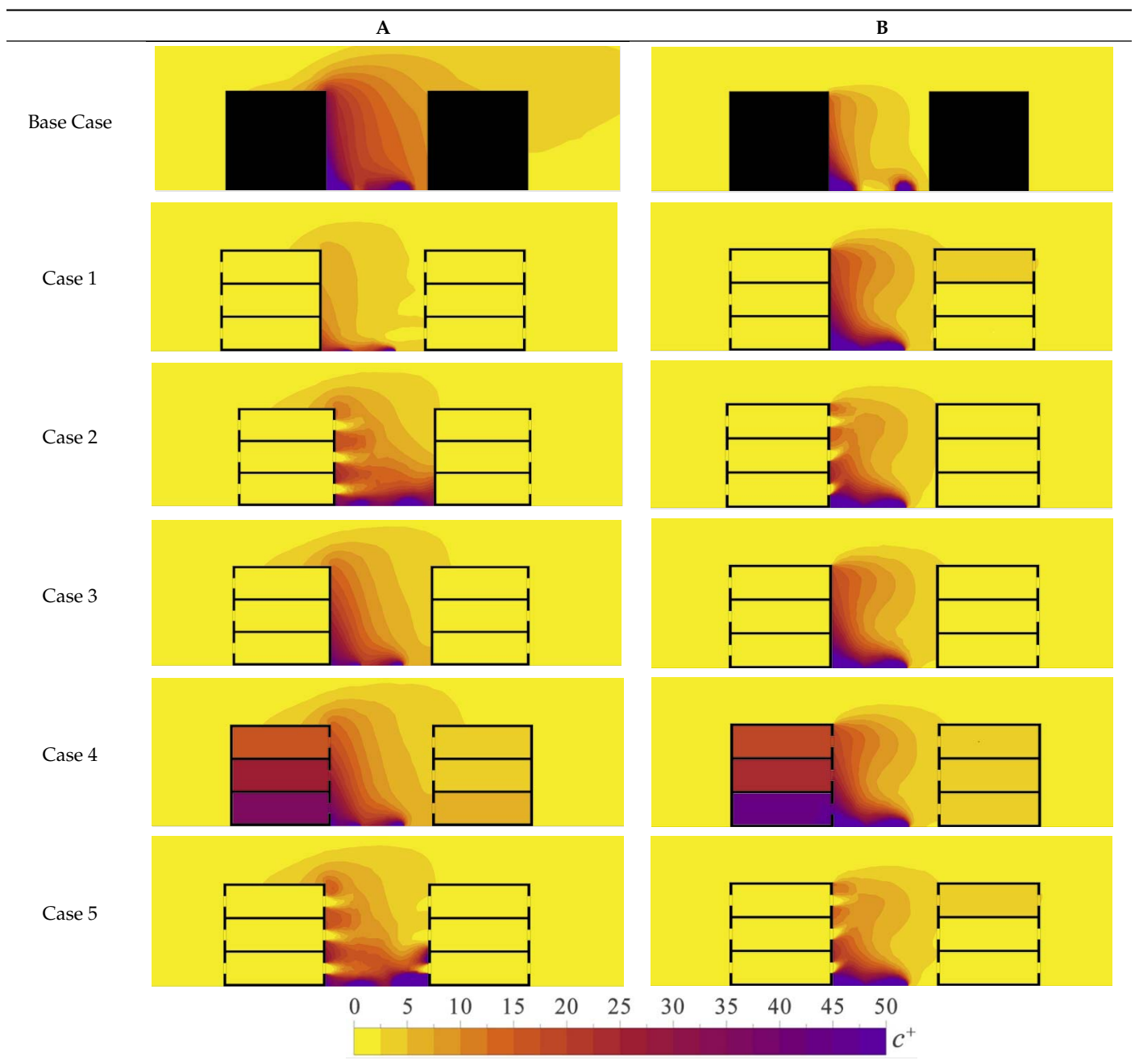
As the research focused on indoor air pollution and the effect of urban configuration, the deviation was considered within the permissible range. The choice of RSM as the turbulence model was justified as the predictions within the region of interest were most close to the experimental data.

### 3. Results and Discussion

Pollution concentration data were analysed at a height of 1.5 m above the floors, which represented the average breathing height of indoor occupants. Similarly, cross-sectional planes through the canyon, at  $X = 0$  m and  $X = 37.5$  m, were also analysed. Table 2 shows the  $c^+$  data along the central ( $X = 0$ ) and side plane ( $X = 37.5$ ). The results were symmetric along the centre of the canyon, and therefore, only one side plane is shown below. It is observed that the indoor  $c^+$  levels are low to almost 0 for all cases, except for Case 4. Higher

pollutant concentration occurs along Wall A regardless of the ventilation or position of the room. When cross ventilation was enabled, the upstream building was ventilated from the windward side, ensuring that pollutants from the canyon were not drawn indoors. Likewise in the downstream building, cross ventilation in Cases 1 and 5 ensures that the air is ventilated from the wind shadow side of the building, i.e., away from the polluted canyon. However, there is a slight increase in  $c^+$  values in rooms UU1 and UU3. This suggests that indoor spaces located on the upper corners of the downstream building were generally ventilated from the canyon side, thereby some amount of infiltration is likely.

**Table 2.** Normalised pollutant concentration along the cross-sectional plane through the canyon; (A) central plane, (B) side plane.



In the case of single-sided ventilation, the quality of indoor air is significantly impacted when air flow occurs from the canyon side. This is evident in Case 4, where high concentra-

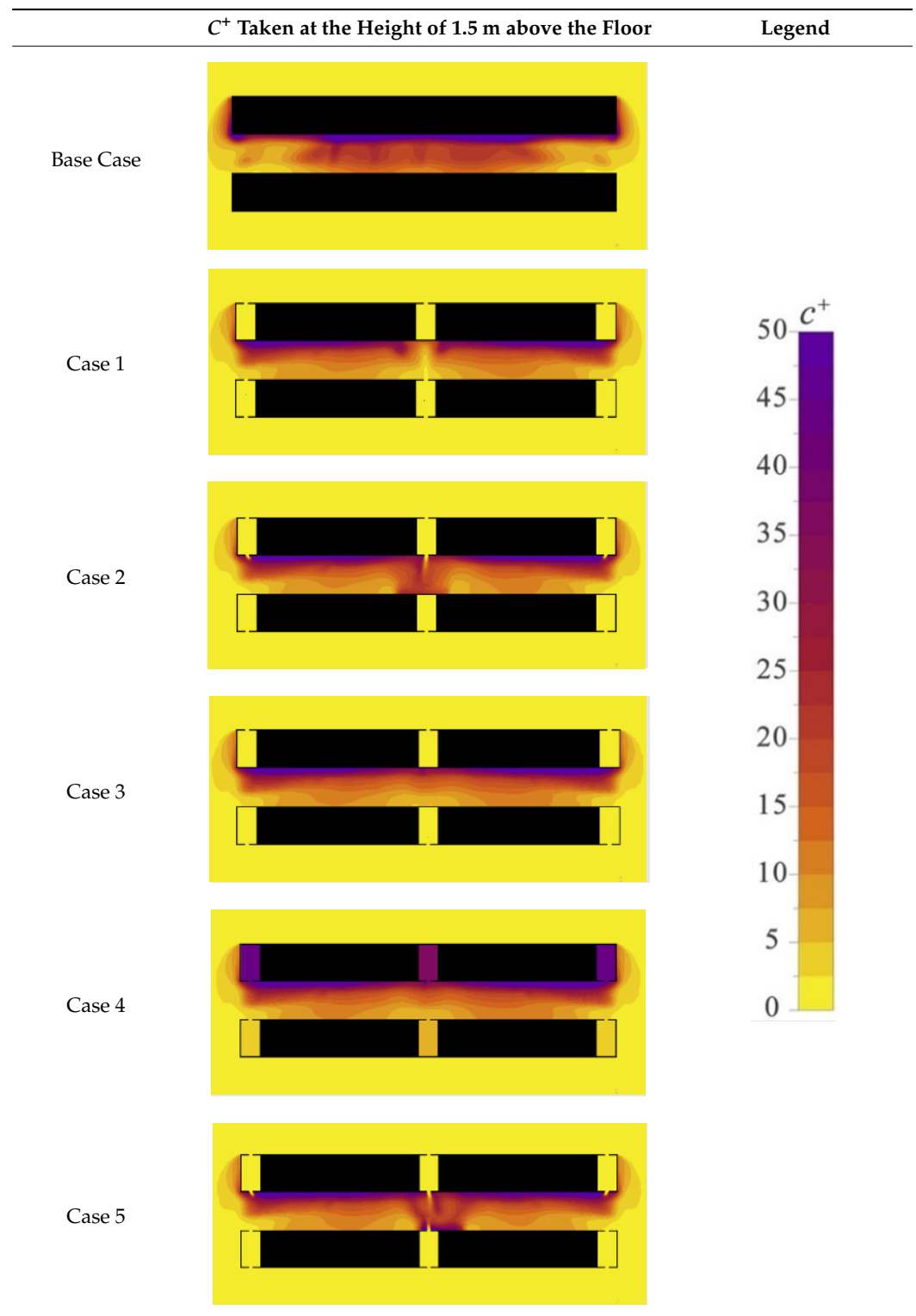
tion of pollution is observed inside both the buildings. Between the two built masses, the downstream building shows lower concentration of indoor pollutants as compared to the upstream building, contrary to general assumption. This can be explained by the clockwise recirculation generated in the canyon, which forces pollutants to accumulate along Wall A. Internal rooms UL2, UM2, and UU2 show higher  $c^+$  values when compared to DL2, DM2, and DU2. Simultaneously, pollution concentration also varies with the floor height. In the upstream building, the indoor concentration level decreases with floor height, while in the downstream building, this variation is only observed for the centrally located spaces. The rooms located towards the ends of the canyon, however, show a reversal in concentration levels. The lower floors record lower  $c^+$  as compared to upper floors (Table 2)

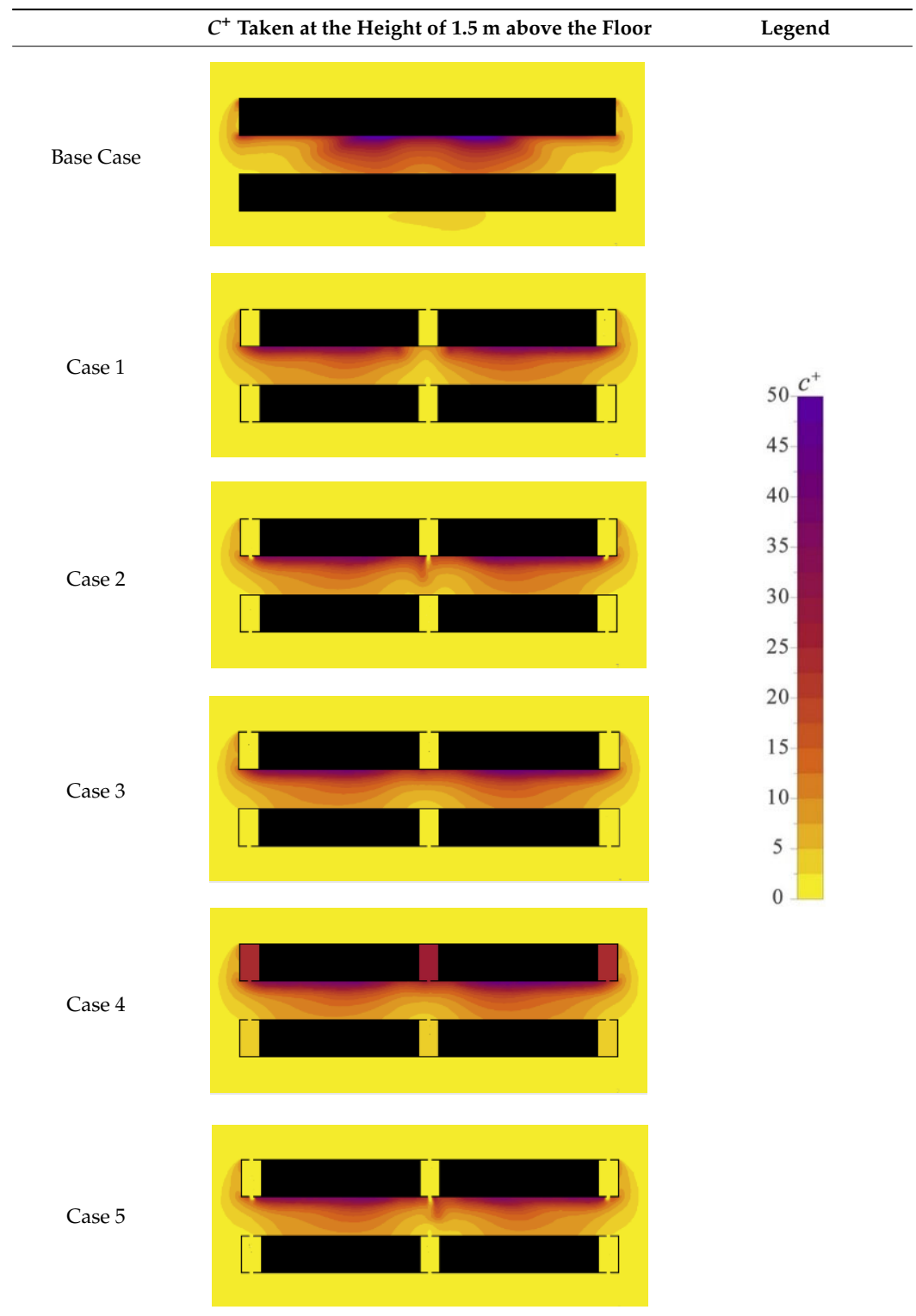
It is interesting to observe that the downstream building is ventilated from the leeward side when cross ventilation was enabled (Cases 1, 4, and 5). This ensures that no pollutants migrate from the canyon side. Recirculation zones generated in the wake of the buildings force the air to rise along the building walls. The clockwise wind flow in the street forces the pollutants to rise along Wall A and flow above the canyon, some of which is recirculated down Wall B.

Table 3 shows the normalised concentration of pollutants extracted at the height of 1.5 m above the ground floor. In the reference case, the swirls generated in the canyon cause concentration to increase along the leeward and side walls of the upstream building. Higher pollutants are observed near the middle of the canyon. Cross flow of air through the internal rooms, such as in Case 1, causes dilution of pollutants in the canyon, although increase in  $c^+$  is observed for some cases near Wall B, such as in Cases 2 and 5. In general, infiltration of pollutants into indoor spaces remains negligible, as air flow inside the room is not from the canyon side. For Case 4, however, the air is drawn into the indoor space from the canyon side, leading to a high concentration of pollutants inside.  $c^+$  values as high as 45 are observed in the upstream rooms (UL1, UL2, and UL3), while values in the range of 3–5 are observed in the downstream rooms (DL1, DL2 and DL3).

Concentration for other cases remain comparatively low. Although the results showed that the cross ventilation minimised or eliminated the built up of pollutants inside the spaces, in practice incorporating such a strategy might not be practical for all types of rooms and buildings. In most cases, there will be several apartments, rooms, or partitions which will dampen the air flow. Hence, further studies should consider a more realistic indoor space instead of an idealised cross flow ventilated space. The results show that incorporating a natural ventilation strategy may not always lead to healthy indoor spaces, in particular, if the ventilated room or space is facing the urban canyon side and employs single-sided ventilation. Future works should consider evaluating the trade-off between natural ventilation and pollutant transmission for these types of spaces.

Pollutant concentration is comparatively lower on the first floor, as shown in Table 4. Recirculating eddies lead to a higher concentration of pollutants near Wall A and around the corners of the upstream building.  $c^+$  contours are symmetric along the central axis, and the highest values are observed at about a distance of 2.5 H from either edge of the building. In Case 1, ventilation of room DM2 from the leeward side forces air into the canyon, diluting the pollutants near Wall B. Similar observations are also made for Cases 4 and 5. Whereas, no such observation is made for cross flow of air through UM2, in the upstream building. On the contrary, a slight increase is observed near Wall B. Case 4 is the most critical configuration, wherein the indoor space is ventilated from the canyon side. Air is drawn from the canyon into the adjoining rooms and a high level of pollution is observed in the upstream building, with an average  $c^+$  value of about 25. Rooms in the downstream building perform relatively better, with  $c^+$  values less than 5. In general, pollution levels on this floor are the same as the ones measured on the ground floor, except for Case 4. While air flows into the internal spaces from the non-canyon side for most configurations, Case 4 shows an exception with air being drawn from the canyon side. This also leads to the intake of pollutants from the canyon, and significantly impacts the performance of the spaces.

**Table 3.** Normalised pollutant concentration at occupants' height on ground floor.

**Table 4.** Pollutant concentration at occupants' height on first floor.

As was indicated previously, pollutant concentration decreases with height, and the same can be observed in the difference between  $c^+$  values between UM2 and UU2. Table 5 shows the pollutant concentration on the second floor, at the height of 8.25 m above ground. Despite the high concentration of pollutants adjacent to Wall A in the base case, internal rooms do not record a significant pollution level. Although a slight increase in  $c^+$  values are observed in the wake of the downstream building for the base case, facilitating air

flow through the building causes dispersion of these pollutants. The pollution distribution pattern follows the pattern similar to that which exists on the lower floors, i.e., negligible  $c^+$  values in the upstream building for all cases, except Case 4. Additionally, the rooms in the downstream building record low levels of pollutant concentration which is almost the same as lower floors.  $c^+$  values of  $\sim 18$  are seen in the spaces UU1, UU2, and UU3, while the upper rooms on the downstream building, DU1, DU2, and DU3 show a value of less than 5.

**Table 5.** Pollutant concentration at occupants' height on second floor.

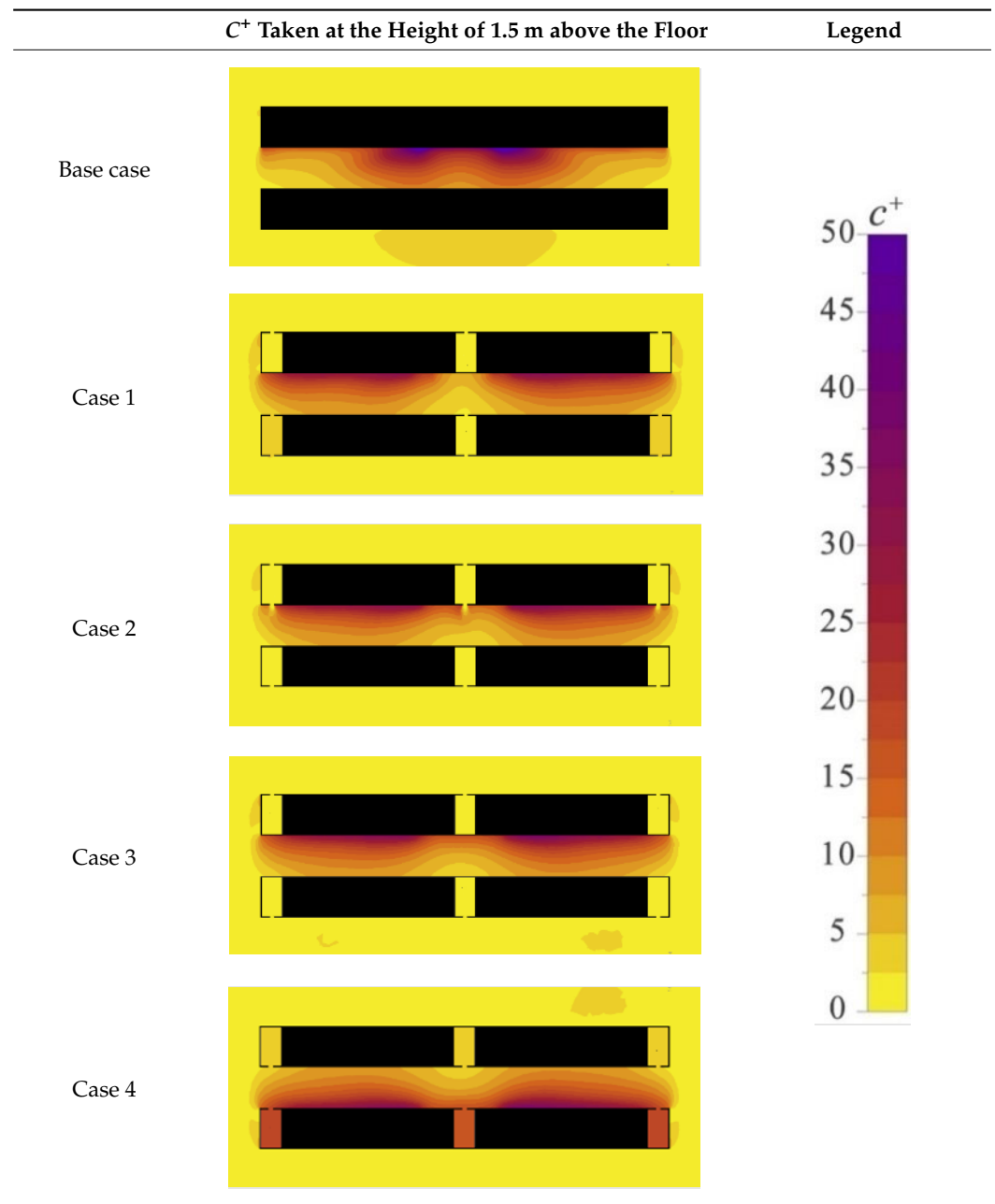
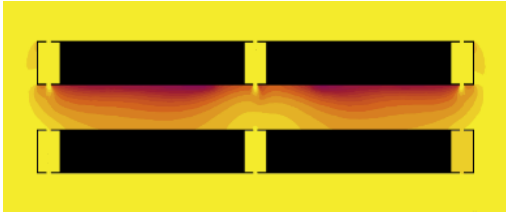


Table 5. Cont.

	$C^+$ Taken at the Height of 1.5 m above the Floor	Legend
Case 5		

A comparison of the average  $c^+$  at the breathing plane is shown in Figure 5. Evidently, except for Case 4, all window opening strategies ensure that the pollution remains low in the indoor regions. The upstream building has a negligible level of pollutants penetrating the indoor spaces for most of the cases. The air flow direction ensures that the spaces are ventilated from the windward side. However, in the critical scenario (Case 4), air flow from the canyon side accumulates the pollutants inside the rooms. Concentration is highest on the ground floor, while there is a drop of about 30–45% on the first floor. Further reductions in the range of 20–30% are observed on the second floor. Additionally, the rooms near the edge of the canyon have a slightly higher pollutant concentration as compared to the centrally located ones. The average values differ by about 10%.

Low levels of infiltration are observed for all cases in the downstream building, arising due to recirculating air flow. Concentration in the range of 1–3 is recorded for all cases, and centrally located rooms are less polluted than the corner ones. Surprisingly, the upper floors are more susceptible to infiltration as compared to lower floors. In Case 1, for instance, DU1 has a 47% higher concentration than DL1. For Case 4, however, concentration in the range of 3–6 is observed, which is nearly a two-fold increase.

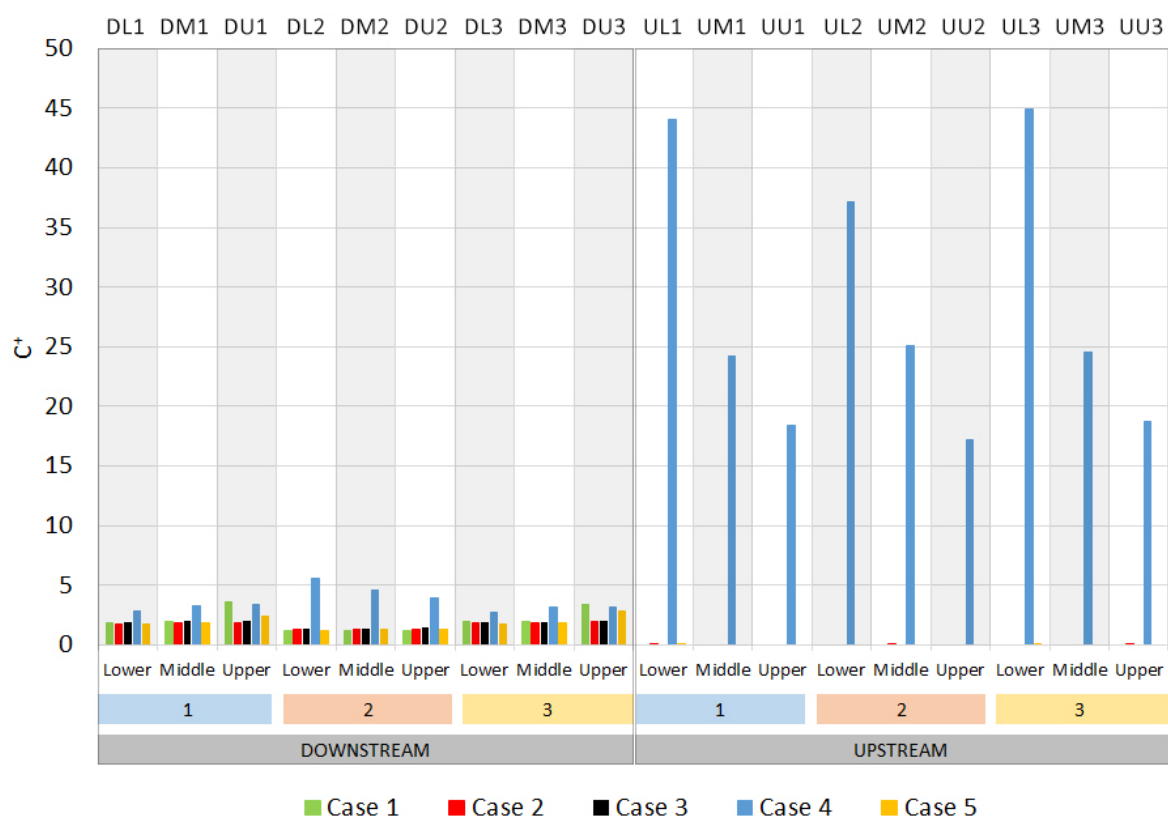


Figure 5. Comparison of average indoor  $c^+$ , measured at occupants' breathing plane.

#### 4. Conclusions and Future Works

The study aimed to identify the transmission characteristics of outdoor pollutants into an indoor environment, using computational modelling in an idealised street canyon. For this purpose, a model was generated in Ansys® (Canonsburg, PA, Pennsylvania) R18.1 similar to the experimental study conducted by Karlsruhe Institute of Technology (Karlsruhe, Germany) [63] and numerical simulation by [44,64,65]. After verification and sensitivity analysis, the archetypal canyon model was modified to consider the indoor environment. The novelty of this study lay in this combination of the indoor and outdoor environment, which has not been tried earlier. Previous studies have either not modelled the indoor environment in a street canyon or have simplified the flow field and missed important parameters. Additionally, the impact of design and microenvironmental parameters on the transmission characteristics and flow field can be studied using this numerical model, including the effect of wind speed, direction, and thermal conditions. Most studies have carried out independent assessment of either indoor or outdoor pollutants, such as performance of HVAC systems or ventilation modes; however, the combined assessment and investigation of factors remains to be explored in detail, including the nature of transmission and finer nuances of air flow.

Investigations in the current study have been directed towards the impact of ventilation strategy on the transmission of outdoor pollutants into indoor spaces. Five window opening strategies were modelled and implemented on an urban canyon with an aspect ratio of 1. Rooms were located at the centre and the far end of the building. The results indicate that single-sided ventilation from the canyon side leads to the accumulation of outdoor pollutants for both the upstream and downstream buildings. Especially, pollution in the upstream building was 10–20 times higher than the downstream building. For other ventilation modes, the upstream building had negligible infiltration of pollutants as the airflow into the interior space was from the windward side—away from the polluting street. Whereas, the downstream building showed constant infiltration of pollutants, albeit in comparatively smaller quantity (in the range of 1–3). It can be concluded that living in the upstream building is usually a safer option than the downstream building; however, occupants in the upstream building must ensure that their spaces are cross ventilated from the windward side. Occupants in the downstream building are usually exposed to a constant pollution level regardless of the ventilation mode.

Future studies should explore the effect of aspect ratio, building shape, and configuration on the air quality and transmission into these spaces. The impact of varying outdoor conditions should be evaluated, which includes the wind speed and direction. The influence of the location, amount, and type of outdoor pollutant sources should also be evaluated. Furthermore, more focus should be given to the indoor environment and indoor pollutant source to help assess inter-unit transmission in urban canyons. The present model did not consider the impact of neighbouring buildings affecting the wind flow patterns around the urban canyon.

**Author Contributions:** Conceptualisation, M.M. and J.C.; methodology, M.M.; software, M.M.; validation, M.M. and J.C.; formal analysis, M.M.; investigation, M.M. and J.C.; resources, J.C.; data curation, M.M.; writing—original draft preparation, M.M.; writing—review and editing, J.C.; visualisation, M.M.; supervision, J.C.; project administration, J.C. Both authors have read and agreed to the published version of the manuscript.

**Funding:** This research received no external funding.

**Institutional Review Board Statement:** Not applicable.

**Informed Consent Statement:** Not applicable.

**Conflicts of Interest:** The authors declare no conflict of interest.

## References

1. Ritchie, H. Indoor Air Pollution. Our World in Data, 16 November 2013. Available online: <https://ourworldindata.org/indoor-air-pollution> (accessed on 5 September 2020).
2. GBD 2017 Risk Factor Collaborators. Global, regional, and national comparative risk assessment of 84 behavioural, environmental and occupational, and metabolic risks or clusters of risks for 195 countries and territories, 1990–2017: A systematic analysis for the Global Burden of Disease Study 2017. *Lancet* **2018**, *392*, 1923–1994. [CrossRef]
3. WHO. *Review of Evidence on Health Aspects of Air Pollution—REVIHAAP Project*; World Health Organization: Geneva, Switzerland, 2013. Available online: <https://www.euro.who.int/en/health-topics/environment-and-health/air-quality/publications/2013/review-of-evidence-on-health-aspects-of-air-pollution-revihaap-project-final-technical-report> (accessed on 9 April 2020).
4. Effects of Air Pollution & Acid Rain on Wildlife. Available online: <http://www.air-quality.org.uk/17.php> (accessed on 9 April 2021).
5. Pope, C.A.; Ezzati, M.; Dockery, D.W. Tradeoffs between income, air pollution and life expectancy: Brief report on the US experience, 1980–2000. *Environ. Res.* **2015**, *142*, 591–593. [CrossRef]
6. Wu, X.; Nethery, R.C.; Sabath, B.; Braun, D.; Dominici, F.; James, C. Exposure to air pollution and COVID-19 mortality in the United States: A nationwide cross-sectional study. *medRxiv Preprint* **2020**. [CrossRef]
7. Coker, E.S.; Cavalli, L.; Fabrizi, E.; Guastella, G.; Lippo, E.; Parisi, M.L.; Pontarollo, N.; Rizzati, M.; Varacca, A.; Vergalli, S. The Effects of Air Pollution on COVID-19 Related Mortality in Northern Italy. *Environ. Resour. Econ.* **2020**, *76*, 611–634. [CrossRef]
8. Copat, C.; Cristaldi, A.; Fiore, M.; Grasso, A.; Zuccarello, P.; Signorelli, S.S.; Conti, G.O.; Ferrante, M. The role of air pollution (PM and NO<sub>2</sub>) in COVID-19 spread and lethality: A systematic review. *Environ. Res.* **2020**, *191*, 110129. [CrossRef] [PubMed]
9. EPA. *Report to Congress on Indoor Air Quality, Volume II: Assessment and Control of Indoor Air Pollution*; EPA: Washington, DC, USA, 1989.
10. Menichini, E.; Iacovella, N.; Monfredini, F.; Turrio-Baldassarri, L. Relationships between indoor and outdoor air pollution by carcinogenic PAHs and PCBs. *Atmos. Environ.* **2007**, *41*, 9518–9529. [CrossRef]
11. Aftermath of Working from Home. University of Southampton. 2020. Available online: <https://www.southampton.ac.uk/news/2020/07/long-term-implications-wfh.page> (accessed on 30 September 2020).
12. Deloitte. The Impact of COVID-19 on Productivity and Wellbeing. 2020. Available online: <https://www2.deloitte.com/uk/en/pages/consulting/articles/working-during-lockdown-impact-of-covid-19-on-productivity-and-wellbeing.html> (accessed on 5 September 2020).
13. Cardiff University. *UK Productivity Could be Improved by a Permanent Shift towards Remote Working*; Cardiff University: Cardiff, UK, 2020. Available online: <https://www.cardiff.ac.uk/news/view/2432442-uk-productivity-could-be-improved-by-a-permanent-shift-towards-remote-working-research-shows> (accessed on 30 September 2020).
14. Spataro, J. The Future of Work. Microsoft 365 Blog. 2020. Available online: <https://www.microsoft.com/en-us/microsoft-365/blog/2020/07/08/future-work-good-challenging-unknown/> (accessed on 5 September 2020).
15. Tien, P.W.; Wei, S.; Liu, T.; Calautit, J.; Darkwa, J.; Wood, C. A Deep Learning Approach Towards the Detection and Recognition of Opening of Windows for Effective Management of Building Ventilation Heat Losses and Reducing Space Heating Demand. *Renew. Energy* **2021**, *177*, 603–625. [CrossRef]
16. Chang, W.R.; Cheng, C.L. Carbon monoxide transport in an enclosed room with sources from a water heater in the adjacent balcony. *Build. Environ.* **2008**, *43*, 861–870. [CrossRef]
17. Park, J.S.; Jee, N.-Y.; Jeong, J.-W. Effects of types of ventilation system on indoor particle concentrations in residential buildings. *Indoor Air* **2014**, *24*, 629–638. [CrossRef]
18. Chen, C.; Zhao, B.; Weschler, C.J. Indoor Exposure to “Outdoor PM<sub>10</sub>”: Assessing Its Influence on the Relationship Between PM<sub>10</sub> and Short-term Mortality in U.S. Cities on JSTOR. *Epidemiology* **2012**, *23*, 870–878. [CrossRef]
19. Chan, A.T. Indoor-outdoor relationships of particulate matter and nitrogen oxides under different outdoor meteorological conditions. *Atmos. Environ.* **2002**, *36*, 1543–1551. [CrossRef]
20. Błaszczyk, E.; Rogula-Kozłowska, W.; Klejnowski, K.; Kubiesa, P.; Fulara, I.; Mielżyńska-Švach, D. Indoor air quality in urban and rural kindergartens: Short-term studies in Silesia, Poland. *Atmos. Health* **2017**, *10*, 1207–1220. [CrossRef]
21. Hassanvand, M.S.; Naddafi, K.; Faridi, S.; Arhami, M.; Nabizadeh, R.; Sowlat, M.H.; Pourpak, Z.; Rastkari, N.; Momeni, F.; Kashani, H.; et al. Indoor/outdoor relationships of PM<sub>10</sub>, PM<sub>2.5</sub>, and PM<sub>1</sub> mass concentrations and their water-soluble ions in a retirement home and a school dormitory. *Atmos. Environ.* **2014**, *82*, 375–382. [CrossRef]
22. Chen, A.; Gall, E.T.; Chang, V.W.C. Indoor and outdoor particulate matter in primary school classrooms with fan-assisted natural ventilation in Singapore. *Environ. Sci. Pollut. Res.* **2016**, *23*, 17613–17624. [CrossRef]
23. Zhao, J.; Birmili, W.; Wehner, B.; Daniels, A.; Weinhold, K.; Wang, L.; Merkel, M.; Kecorius, S.; Tuch, T.; Franck, U.; et al. Particle Mass Concentrations and Number Size Distributions in 40 Homes in Germany: Indoor-to-Outdoor Relationships, Diurnal and Seasonal Variation. *Aerosol Air Qual. Res.* **2020**, *20*, 576–589. [CrossRef]
24. Chiesa, M.; Urgnani, R.; Marzuoli, R.; Finco, A.; Gerosa, G. Site- and house-specific and meteorological factors influencing exchange of particles between outdoor and indoor domestic environments. *Build. Environ.* **2019**, *160*, 106181. [CrossRef]
25. Wang, F.; Meng, D.; Li, X.; Tan, J. Indoor-outdoor relationships of PM<sub>2.5</sub> in four residential dwellings in winter in the Yangtze River Delta, China. *Environ. Pollut.* **2016**, *215*, 280–289. [CrossRef] [PubMed]

26. Rim, D.; Gall, E.T.; Kim, J.B.; Bae, G.N. Particulate matter in urban nursery schools: A case study of Seoul, Korea during winter months. *Build. Environ.* **2017**, *119*, 1–10. [[CrossRef](#)]
27. Niu, J.; Tung, T.C.W. On-site quantification of re-entry ratio of ventilation exhausts in multi-family residential buildings and implications. *Indoor Air* **2007**, *18*, 12–26. [[CrossRef](#)] [[PubMed](#)]
28. Mao, J.; Gao, N. The airborne transmission of infection between flats in high-rise residential buildings: A review. *Build. Environ.* **2015**, *94*, 516–531. [[CrossRef](#)]
29. Tippayawong, N.; Khuntong, P.; Nitatwichit, C.; Khunatorn, Y.; Tantakitti, C. Indoor/outdoor relationships of size-resolved particle concentrations in naturally ventilated school environments. *Build. Environ.* **2009**, *44*, 188–197. [[CrossRef](#)]
30. Lv, Y.; Wang, H.; Wei, S.; Zhang, L.; Zhao, Q. The Correlation between Indoor and Outdoor Particulate Matter of Different Building Types in Daqing, China. *Procedia Eng.* **2017**, *205*, 360–367. [[CrossRef](#)]
31. Gupta, A.; David Cheong, K.W. Physical characterization of particulate matter and ambient meteorological parameters at different indoor-outdoor locations in Singapore. *Build. Environ.* **2007**, *42*, 237–245. [[CrossRef](#)]
32. Chithra, V.S.; Shiva Nagendra, S.M. Impact of outdoor meteorology on indoor PM10, PM2.5 and PM1 concentrations in a naturally ventilated classroom. *Urban Clim.* **2014**, *10*, 77–91. [[CrossRef](#)]
33. Orza, J.A.G.; Cabello, M.; Lidón, V.; Martínez, J. Contribution of resuspension to particulate matter inmission levels in SE Spain. *J. Arid Environ.* **2011**, *75*, 545–554. [[CrossRef](#)]
34. He, L.; Hang, J.; Wang, X.; Lin, B.; Li, X.; Lan, G. Numerical investigations of flow and passive pollutant exposure in high-rise deep street canyons with various street aspect ratios and viaduct settings. *Sci. Total Environ.* **2017**, *584–585*, 189–206. [[CrossRef](#)]
35. Tominaga, Y.; Stathopoulos, T. Ten questions concerning modeling of near-field pollutant dispersion in the built environment. *Build. Environ.* **2016**, *105*, 390–402. [[CrossRef](#)]
36. Ai, Z.T.; Mak, C.M. *From Street Canyon Microclimate to Indoor Environmental Quality in Naturally Ventilated Urban Buildings: Issues and Possibilities for Improvement*; Elsevier: Amsterdam, The Netherlands, 2015; Volume 94, pp. 489–503.
37. Yuan, C. Improving Air Quality by Understanding the Relationship Between Air Pollutant Dispersion and Building Morphologies. In *Springer Briefs in Architectural Design and Technology*; Springer: Berlin/Heidelberg, Germany, 2018; pp. 117–140.
38. Salim, S.M.; Buccolieri, R.; Chan, A.; Di Sabatino, S. Numerical simulation of atmospheric pollutant dispersion in an urban street canyon: Comparison between RANS and LES. *J. Wind Eng. Ind. Aerodyn.* **2011**, *99*, 103–113. [[CrossRef](#)]
39. Hong, B.; Qin, H.; Lin, B. Prediction of wind environment and indoor/outdoor relationships for PM2.5 in different building-tree grouping patterns. *Atmosphere* **2018**, *9*, 39. [[CrossRef](#)]
40. Rai, P.K.; Panda, L.L.S. Dust capturing potential and air pollution tolerance index (APTI) of some road side tree vegetation in Aizawl, Mizoram, India: An Indo-Burma hot spot region. *Air Qual. Atmos. Health* **2014**, *7*, 93–101. [[CrossRef](#)]
41. Tong, Z.; Chen, Y.; Malkawi, A.; Adamkiewicz, G.; Spengler, J.D. Quantifying the impact of traffic-related air pollution on the indoor air quality of a naturally ventilated building. *Environ. Int.* **2016**, *89–90*, 138–146. [[CrossRef](#)]
42. Yang, F.; Kang, Y.; Gao, Y.; Zhong, K. Numerical simulations of the effect of outdoor pollutants on indoor air quality of buildings next to a street canyon. *Build. Environ.* **2015**, *87*, 10–22. [[CrossRef](#)]
43. Peng, Y.; Ma, X.; Zhao, F.; Liu, C.; Mei, S. Wind driven natural ventilation and pollutant dispersion in the dense street canyons: Wind Opening Percentage and its effects. *Procedia Eng.* **2017**, *205*, 415–422. [[CrossRef](#)]
44. Hong, B.; Qin, H.; Jiang, R.; Xu, M.; Niu, J. How Outdoor Trees Affect Indoor Particulate Matter Dispersion: CFD Simulations in a Naturally Ventilated Auditorium. *Int. J. Environ. Res. Public Health* **2018**, *15*, 2862. [[CrossRef](#)]
45. Wang, B.; Hang, J.; Buccolieri, R.; Yang, X.; Yang, H.; Quarta, F. Impact of indoor-outdoor temperature differences on dispersion of gaseous pollutant and particles in idealized street canyons with and without viaduct settings. In *Building Simulation*; Tsinghua University Press: Beijing, China, 2019; Volume 12, pp. 285–297. [[CrossRef](#)]
46. Hassan, A.M.; ELMokadem, A.A.; Megahed, N.A.; Abo Eleinen, O.M. Urban morphology as a passive strategy in promoting outdoor air quality. *J. Build. Eng.* **2020**, *29*, 101204. [[CrossRef](#)]
47. Gousseau, P.; Blocken, B.; Stathopoulos, T.; van Heijst, G.J.F. CFD simulation of near-field pollutant dispersion on a high-resolution grid: A case study by LES and RANS for a building group in downtown Montreal. *Atmos. Environ.* **2011**, *45*, 428–438. [[CrossRef](#)]
48. Huang, J.; Jones, P.; Zhang, A.; Hou, S.S.; Hang, J.; Spengler, J.D. Outdoor Airborne Transmission of Coronavirus Among Apartments in High-Density Cities. *Front. Built Environ.* **2021**, *7*, 48. [[CrossRef](#)]
49. Liu, X.; Peng, Z.; Liu, X.; Zhou, R. Dispersion Characteristics of Hazardous Gas and Exposure Risk Assessment in a Multiroom Building Environment. *Int. J. Environ. Res. Public Health* **2020**, *17*, 199. [[CrossRef](#)] [[PubMed](#)]
50. Yang, F.; Zhong, K.; Chen, Y.; Kang, Y. Simulations of the impacts of building height layout on air quality in natural-ventilated rooms around street canyons. *Environ. Sci. Pollut. Res.* **2017**, *24*, 23620–23635. [[CrossRef](#)]
51. Wang, J.; Huo, Q.; Zhang, T.; Wang, S.; Battaglia, F. Numerical investigation of gaseous pollutant cross-transmission for single-sided natural ventilation driven by buoyancy and wind. *Build. Environ.* **2020**, *172*, 106705. [[CrossRef](#)]
52. Mei, S.J.; Luo, Z.; Zhao, F.Y.; Wang, H.Q. Street canyon ventilation and airborne pollutant dispersion: 2-D versus 3-D CFD simulations. *Sustain. Cities Soc.* **2019**, *50*, 101700. [[CrossRef](#)]
53. Tominaga, Y.; Stathopoulos, T. CFD modeling of pollution dispersion in a street canyon: Comparison between LES and RANS. *J. Wind Eng. Ind. Aerodyn.* **2011**, *99*, 340–348. [[CrossRef](#)]
54. Wang, Y.; Zhao, T.; Cao, Z.; Zhai, C.; Wu, S.; Zhang, C.; Zhang, Q.; Lv, W. The influence of indoor thermal conditions on ventilation flow and pollutant dispersion in downstream industrial workshop. *Build. Environ.* **2021**, *187*, 107400. [[CrossRef](#)]

55. Gromke, C.; Ruck, B. Pollutant Concentrations in Street Canyons of Different Aspect Ratio with Avenues of Trees for Various Wind Directions. *Bound.-Layer Meteorol.* **2012**, *144*, 41–64. [[CrossRef](#)]
56. Milner, J.; Vardoulakis, S.; Chalabi, Z.; Wilkinson, P. Modelling inhalation exposure to combustion-related air pollutants in residential buildings: Application to health impact assessment. *Environ. Int.* **2011**, *37*, 268–279. [[CrossRef](#)] [[PubMed](#)]
57. Blocken, B. 50 years of Computational Wind Engineering: Past, present and future. *J. Wind Eng. Ind. Aerodyn.* **2014**, *129*, 69–102. [[CrossRef](#)]
58. Chaouat, B. The State of the Art of Hybrid RANS/LES Modeling for the Simulation of Turbulent Flows. *Flow Turbul. Combust.* **2017**, *99*, 279–327. [[CrossRef](#)]
59. Gromke, C.; Buccolieri, R.; Di Sabatino, S.; Ruck, B. Dispersion study in a street canyon with tree planting by means of wind tunnel and numerical investigations—Evaluation of CFD data with experimental data. *Atmos. Environ.* **2008**, *42*, 8640–8650. [[CrossRef](#)]
60. Yazid, A.W.M.; Sidik, N.A.C.; Salim, S.M.; Saqr, K.M. A review on the flow structure and pollutant dispersion in urban street canyons for urban planning strategies. *Simulation* **2014**, *90*, 892–916. [[CrossRef](#)]
61. Gan, C.J.; Salim, S.M. Numerical analysis of fluid-structure interaction between wind flow and trees. *Lect. Notes Eng. Comput. Sci.* **2014**, *2*, 1218–1223.
62. Jeanjean, A.P.R.; Hinchliffe, G.; McMullan, W.A.; Monks, P.S.; Leigh, R.J. A CFD study on the effectiveness of trees to disperse road traffic emissions at a city scale. *Atmos. Environ.* **2015**, *120*, 1–14. [[CrossRef](#)]
63. Karlsruhe Institute of Technology CODASC. Concentration Data of Street Canyons. Laboratory of Building- and Environmental Aerodynamics. 2008. Available online: <https://www.windforschung.de/CODASC.htm> (accessed on 13 October 2020).
64. Salim, S.M. Computational Study of Wind Flow and Pollutant Dispersion Near Tree Canopies. Ph.D. Thesis, University of Nottingham, Nottingham, UK, 2011.
65. Kang, G.; Kim, J.-J.; Kim, D.-J.; Choi, W.; Park, S.-J. Development of a computational fluid dynamics model with tree drag parameterizations: {Application} to pedestrian wind comfort in an urban area. *Build. Environ.* **2017**, *124*, 209–218. [[CrossRef](#)]
66. Buccolieri, R.; Salim, S.M.; Leo, L.S.; Di Sabatino, S.; Chan, A.; Ielpo, P.; de Gennaro, G.; Gromke, C. Analysis of local scale tree-atmosphere interaction on pollutant concentration in idealized street canyons and application to a real urban junction. *Atmos. Environ.* **2011**, *45*, 1702–1713. [[CrossRef](#)]